Multinary Intermetallics from Molten Al. Synthesis of $SmNiAl_4Ge_2$ and $YNiAl_4Ge_2$. Possible Spin Frustration in Separated Triangular Sm^{3+} Layers

B. Sieve,[†] X. Chen,[†] J. Cowen,[‡,§] P. Larson,[‡] S. D. Mahanti,[‡] and M. G. Kanatzidis*[,†]

Department of Chemistry and Department of Physics and Astronomy, Michigan State University, East Lansing, Michigan 48824

Received March 15, 1999. Revised Manuscript Received June 8, 1999

$SmNiAl_4Ge_2$ crystallizes from molten Al containing Sm, Ni, and Ge. The compound crystallizes in the rhomohedral space group $R3m$ with $a = 4.1121(6)$ Å, $c = 31.109(6)$ Å, and $V = 455.5(1)$ Å^3. The $YNiAl_4Ge_2$ analogue is also stable. The crystal structure consists of layers of $[NiAl_4Ge_2]^{3-}$ separated by monolayers of hexagonally close-packed Sm^{3+} ions. The Ni atoms are surrounded by eight Al atoms in the structure. Each Sm atom has an octahedral environment of six Ge atoms. The magnetism of $SmNiAl_4Ge_2$ is unusual, possibly reflecting the presence of geometrical spin frustration. The magnetization exhibits a well-defined hysteresis loop, without signs of ferromagnetism. It also exhibits irreversibility in the field-cooled and zero-field-cooled magnetization but without the typical characteristic spin glass behavior.

Introduction

The use of molten solids as reaction media for exploratory synthesis has accelerated during the past decade with a variety of flux techniques becoming increasingly prominent. These involve predominantly molten salts such as alkali metal and alkaline earth metal halides,[1] alkali polychalcogenides,[2] and polychalcophosphates,[3] metal oxide and borate fluxes,[4] and to a lesser extent, molten metal fluxes such as Sn[5] and Al.[6] Recently, we became interested in exploring new synthetic pathways for solid-state compounds containing main group elements from groups 13 and 14. We decided to examine the utility of molten Al[7,8] and Ga[9] in providing useful synthetic routes to such materials. We already reported on the use of Al as a solvent to synthesize ternary and quaternary metal aluminide silicides, as well as the use of Ga to prepare $SmNiSi_3$ and Sm_2NiGa_{12}. Aluminum fluxes have been used to prepare borides[10] at very high temperature (>1400 °C) and aluminides, but very little has been done with tetrelides (Si, Ge, Sn). Because molten Al dissolves Si without forming a compound,[11] we reasoned it might serve as a convenient solvent for delivery of Si atoms in a reaction. Therefore, molten Al should serve as a useful medium for silicide synthesis, particularly for exploring new systems. We find that crystals of various metal aluminum silicides grow easily in Al melt below 1000 °C and so far we have discovered a large number of members of a new class of silicides. We recently reported the formation of the new family $Ln_2Al_3Si_2$ (Ln = Dy, Ho, Er, Tm)[7] and $Sm_2Ni(Ni_xSi_{1-x})Al_4Si_6$ (x = 0.18−0.27)[8] in Al flux. Here we report on the use of molten Al in the synthesis of intermetallic germanides. Namely, we describe the synthesis, structure, and magnetic properties of a new quaternary aluminum germanide, $SmNiAl_4Ge_2$, which crystallizes from molten Al in a new structure type.

* To whom correspondence should be addressed.
[†] Department of Chemistry.
[‡] Department of Physics and Astronomy.
[§] Deceased.

(1) Carpenter, J. D.; Hwu, S. J. *Inorg. Chem.* **1995**, *34*(18), 4647−4651. (b) Etheredge, K. M. S.; Hwu, S. J. *Inorg. Chem.* **1995**, *34*(6), 1495−1499. (c) Gencer, F.; Abell, J. S. *J. Cryst. Growth.* **1991**, *112*(2−3), 337−342. (d) Chen, C. K.; Wanklyn, B. M. *J. Cryst. Growth.* **1989**, *96*(3), 547−551. (e) Lee, S.; Fischer, E.; Czerniak, J.; Nagasundaram, N. *J. Alloys Compd.* **1993**, *197*(1), 1−5.

(2) Kanatzidis, M. G.; Sutorik, A. *Progr. Inorg. Chem.* **1995**, *34*, 151−265.

(3) Kanatzidis, M. G. *Curr. Opin. Solid State Mater. Sci.* **1997**, *2*, 139−149.

(4) (a) Utzolino, A.; Bluhm, K. *Z. Naturforsch., B: Chem. Sci.* **1996**, *51*(3), 305−308. (b) Schaefer, J.; Bluhm, K. *Z. Anorg. Allg. Chem.* **1994**, *620*(9), 1578−1582. (c) Luce, J. L.; Schaffers, K. I.; Keszler, D. A. *Inorg. Chem.* **1994**, *33*(11), 2453−2455.

(5) (a) Canfield, P. C.; Fisk, Z. *Philos. Mag. B* **1992**, *65*(6), 1117−1123. (b) Le Senechal, C.; Pivan, J. Y.; Deputier, S.; Guerin, R. *Mater. Res. Bull.* **1998**, *33*(6), 887−902. (c) Kaiser, P.; Jeitschko, W. *J. Solid State Chem.* **1996**, *124*(2), 346−352. (d) Ebel, T.; Jeitschko, W. *J. Solid State Chem.* **1995**, *116*(2), 307−313.

(6) (a) Niemann, S.; Jeitschko, W. *J. Solid State Chem.* **1995**, *114*, 337−341. (b) *Z. Kristallogr.* **1995**, *210*, 338−341. (c) *J. Solid State Chem.* **1995**, *116*, 131−135. (d) *J. Alloys Compd.* **1995**, *221*, 235−239.

(7) Chen, X. Z.; Sieve, B.; Henning, R.; Schultz, A. J.; Brazis, P.; Kannewurf, C. R.; Cowen, J. A.; Crosby, R.; Kanatzidis, M. G. *Angew. Chem., Intl. Ed. Engl.* **1999**, *38*, 693−696.

(8) Chen, X. Z.; Sportouch, S.; Sieve, B.; Brazis, P.; Kannewurf, C. R.; Cowen, J. A.; Patschke, R.; Kanatzidis, M. G. *Chem. Mater.* **1998**, *10*, 3202−3211.

(9) Chen, X. Z.; Larson, P.; Sportouch, S.; Brazis, P.; Mahanti, S. D.; Kannewurf, C. R.; Kanatzidis, M. G. *Chem. Mater.* **1999**, *11*, 75−83.

(10) (a) *Boron and Refractory Borides*; Matkovich, V. I., Ed.; Springer-Verlag: Berlin 1977; see also references therein. (b) Okada, S.; Yu, Y.; Lundström, T.; Kudou, K.; Tanaka, T. *Jpn. J. Appl. Phys.* **1996**, *35*, 4718−4723. (c) Okada, S.; Kudou, K.; Yu, Y.; Lundstrom, T. *Jpn. J. Appl. Phys.* **1994**, *33*(5A), 2663−2666.

(11) Massalski, T. B. *Binary Alloy Phase Diagrams*; Scott, W., Jr., Ed.; ASM International Publisher: Materials Park, OH, 1990.

10.1021/cm990155+ CCC: $18.00
Published on Web 08/31/1999

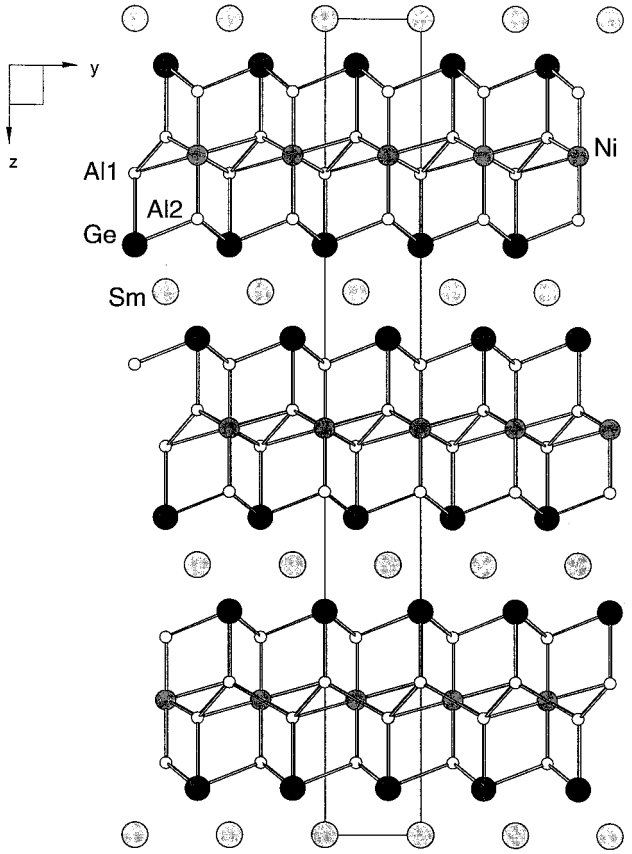

Figure 1. The structure of $SmNiAl_4Ge_2$ viewed down the *a*-axis. Small open circles are Al atoms.

Results and Discussion

Germanium is even more soluble in aluminum than is Si. On the basis of this, we set out to demonstrate the utility of aluminum flux for germanide synthesis and to prepare Ge analogues of $Sm_2Ni(Ni_xSi_{1-x})Al_4Si_6$. The aluminum flux approach can be extended to germanium compounds, however, isostructural analogues to corresponding Si compounds are rarely observed. The $SmNiAl_4Ge_2$ forms as well-shaped hexagonal plates when the Sm/Ni/Ge react in molten Al in the ratio 1:1:*n* ($n = 2-5$). When the Sm/Ni/Ge ratio is 2:1:*n*, a new tetragonal phase Sm_2NiAl_3Ge is obtained,[12] implying strongly that in this system alone the synthetic chemistry is relatively rich.

The $SmNiAl_4Ge_2$ adopts a well-ordered rhombohedral structure with $[NiAl_4Ge_2]$ layers separated by Sm atoms (see Figure 1). The layers possess trigonal symmetry and are made of a continuous network of Al and Ge atoms. Each layer is approximately 8 Å thick and contains seven atomic layers of Ge and Al in the stacking sequence Ge−Al−Al−Ni−Al−Al−Ge of the packing motif ABABCBC. This generates Al−Al bonding and a puckered aluminum layer in the middle of the $[NiAl_4Ge_2]$ layer with an As-type structure. This structure type requires that both surfaces of each $[NiAl_4Ge_2]$ layer be terminated with Ge atoms (see Figure 2A). A closer look at the structure reveals umbrella-like Ge atoms which require all Ge−Al bonds to be directed on the same side of the Ge atom and toward the center of the $[NiAl_4Ge_2]$ layer (see Figure 2B). Presumably, the

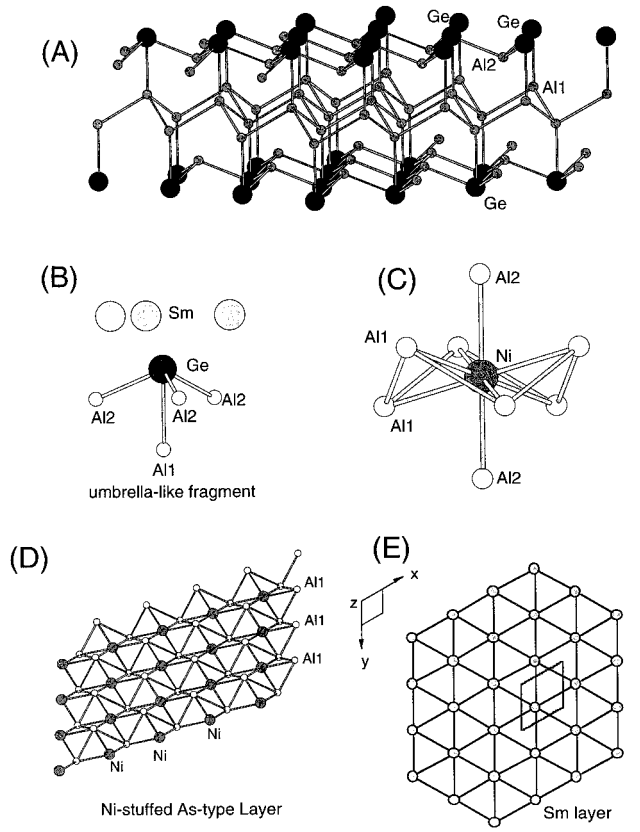

Figure 2. (A) The Ni-stuffed As-type layer of Al atoms found in the middle of the $[NiAl_4Ge_2]$ layers. (B) Immediate coordination environment of Ge (umbrella like) and Ni (eight coordinate). (C) Immediate coordination environment of Ni. (D) View of the middle section of the $[NiAl_4Ge_2]$ layer showing only the puckered $NiAL_2$ plane. (E) The triangular layer of Sm atoms.

opposite side of the Ge atoms involves lone pairs of electrons interacting with the Sm atoms. The umbrella-type geometry for Ge is similar to that found in $CaAl_2Ge_2$.[13]

The puckered Al-hexagons (cyclohexane chair conformation) in the As-type layer are large enough (Al−Al bond lengths of 2.749 Å) to accommodate the relatively small Ni atoms. Each Ni atom is thus surrounded not only by the six Al atoms in the As-type layer but also by two Al atoms above and below this layer to achieve an eight-coordinate environment with Ni−Al bonds ranging from 2.40 to 2.47 Å (see Figures 2C and D).

The Sm atoms occur in planes perpendicular to the *c*-axis. They close pack so that they form a perfect triangular net. The triangles are equilateral with Sm−Sm edges of 4.12 Å. The spacing between the Sm layers is 10 Å. Therefore, the well-separated planar triangular arrays of paramagnetic Sm atoms have the potential of creating spin frustration, which could lead to unusual magnetic phenomena.[14]

It would be interesting to consider how the valence electrons are distributed in $SmNiAl_4Ge_2$. The assumption that the formal charge of Sm atoms would be 3+ is reasonable because they are the most electropositive atoms. This is also supported experimentally by the

(12) Sieve, B.; Kanatzidis, M. G. To be submitted for publication.

(13) Gladyshevskii, E. I.; Kripyakevich, P. I.; Bodak, O. I. *Ukr. Phys. J.* **1967**, *12*, 447−452.

(14) Schiffer, P.; Ramirez, A. P. *Comments Condens. Mater. Phys.* **1996**, *18*, 21−50 and references therein.

magnetic susceptibility measurements that are consistent with Sm^{3+} (see below). Furthermore, in related compounds of this type such as $Sm_2Ni(Ni_xSi_{1-x})Al_4Si_6$ [8] and $SmNiSi_3$,[9] the lanthanide atom occurs in the 3+ state. Therefore, we can assign the electron distribution as $Sm^{3+}[NiAl_4Ge_2]^{3-}$. Ni however, is more electronegative than Al and only slightly more electronegative than Ge (1.9 vs 1.8 in Pauling scale) and it is likely that Ni would accept electrons from Sm and Al and perhaps even from Ge. On the basis of electronegativity arguments, the formal charge on Ni might be expected to be either 0 or even negative. This will result in an electron-rich d^{10} or even s^2d^{10} configuration for Ni, giving a diamagnetic center.

To further explore the electronic structure of $SmNiAl_4Ge_2$ we performed ab initio electronic band structure calculations using density functional theory (DFT).[15] To avoid, however, the difficulties associated with the presence of incomplete f-shells in such calculations, we replaced Sm with Y. In fact, the isostructural $YNiAl_4Ge_2$ forms under analogous synthetic conditions. The total and partial density of states (DOS) are given in Figure 3A. The Fermi level crosses several bands and falls within a deep valley in the DOS suggesting that $YNiAl_4Ge_2$ is a metal or a semimetal.[16] The Y s, p, and d orbital contribution to the DOS is given in Figure 3B and it can be seen that it is negligible below the Fermi level consistent with a 3+ formal charge for the rare earth metal. In contrast, the d orbitals of Ni are almost fully occupied with electrons because they lie significantly below the Fermi energy, suggesting a reduced state for this atom (Figure 3C). Near the Fermi level the predominant contributions are from Al and Ge s and p orbitals.[17]

Magnetic Properties. The most intriguing property of $SmNiAl_4Ge_2$ is its magnetism. The ideal triangular arrangement of Sm atoms in parallel planes separated by a 10 Å spacing suggests that nearest neighbor magnetic Sm−Sm interactions within the plane will be substantially stronger than those between planes. This could set the stage for an interesting case of geometrical spin-frustration.[18] In ideal two-dimensional triangular spin lattices the magnetic ground state is degenerate and unstable, and as a consequence, unusual magnetic

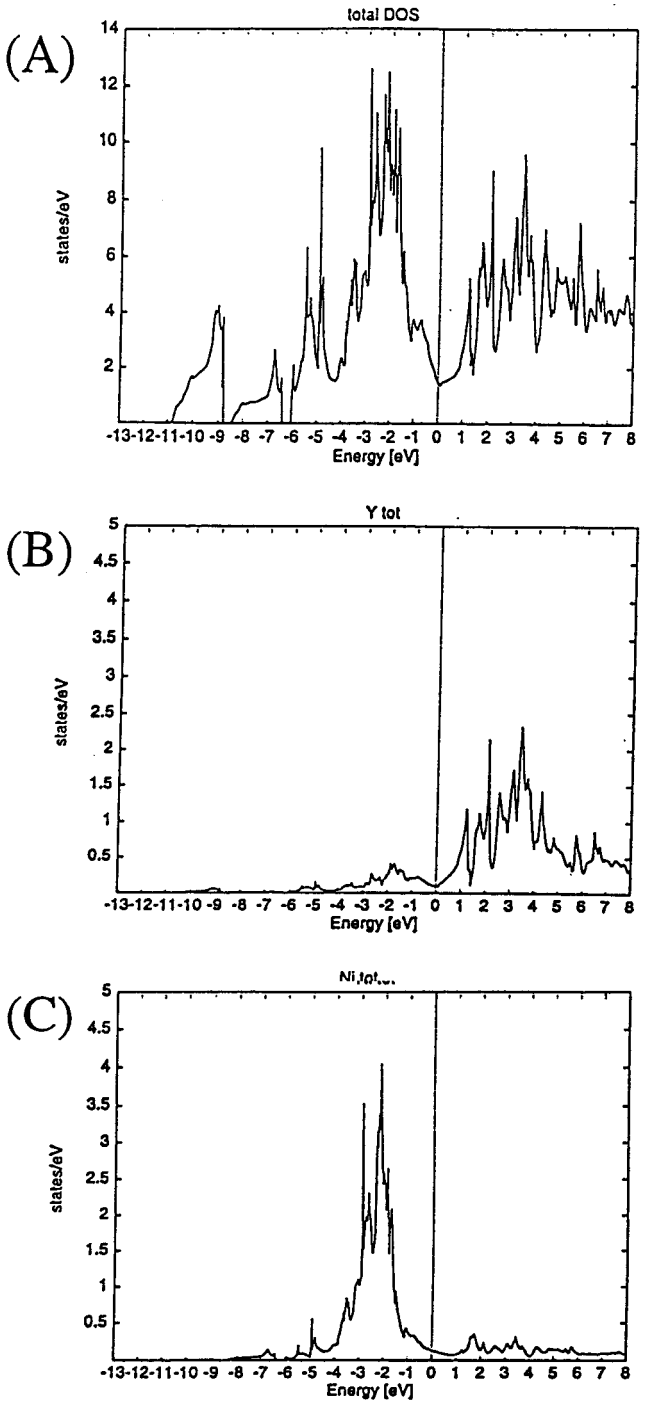

Figure 3. (A) Calculated total DOS for $YNiAl_4Ge_2$. (B) Partial DOS for Y, s, p, and d orbitals in $YNiAl_4Ge_2$. (C) The Ni atom s, p, and d orbital contribution to the DOS. The sharp narrow peak between −1 and −4 eV is mainly Ni d orbitals.

phenomena can arise.[13] The magnetization of $SmNiAl_4Ge_2$ was studied as a function of magnetic field and temperature. The compound exhibits a broad maximum in the zero-field-cooled susceptibility (see Figure 4A), and the onset of irreversibility between zero-field-cooled and field-cooled magnetization which commences already at ∼300 K. A well-defined hysteresis loop is observed (see Figure 4B), in which the magnetization locally saturates at 10 000 G. Both of these properties could be characteristic of disordered or spin-glass systems. The compound, however, cannot be classified unequivocally as a spin glass because it fails several

(15) Blaha, P.; Schwarz, K.; Luitz, J., WIEN97: A Full Potential Linearized Augmented Plane Wave Package for Calculating Crystal Properties, Vienna University of Technology, Getreidemarkt 9/158, A-1060 Vienna, Austria. (b) Perdew, J. P.; Burke, S.; Ernzerhof, M. *Phys. Rev. Lett.* **1996**, *77*, 3865.

(16) Thermopower measurements between 80 and 400 K show a Seebeck coefficient of +5 μV/K typical of a p-type metal system.

(17) It is interesting, however, that the structure of $[Al_4Ge_2]$ layer can be rationalized in terms of the Zintl concept, especially if we assign to it a 4-charge. In this fashion the tetrahedral geometry of Al could be explained by virtue of each accepting one electron, presumably from Sm and Ni, which would require Ni to assume a +1 oxidation state.

(18) In an ideal geometrically frustrated Heisenberg spin system without disorder, the ground states are not necessarily separated by energy barriers, leading to a continuum of equivalent ground states. The ground state character of geometrically frustrated magnetic systems is an unsolved problem in condensed matter physics and has been an active area of theoretical research. Both the nature of the ground state in different systems (e.g., lattice type, spin size, and dimensionality) and the process of relaxation between metastable states under the influence of quantum and thermal perturbations have been the subject of controversy. Although much theoretical effort has been directed toward these issues, the problems are difficult to resolve either analytically or computationally (due to the high degeneracy of ground states), and there is a strong need for complementary experimental work to focus the theoretical effort.

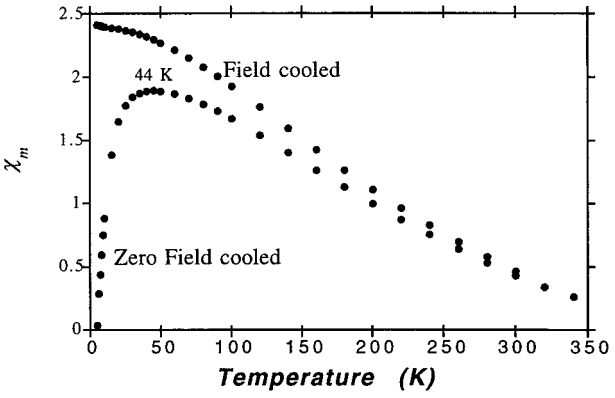

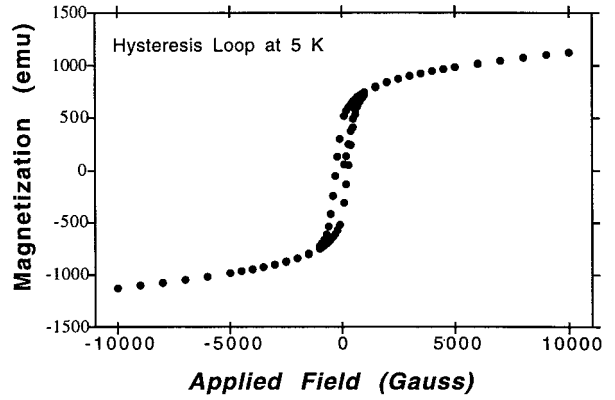

Figure 4. (A) χ_m vs T plot for a polycrystalline sample of $SmNiAl_4Ge_2$. (B) Hysteresis loop obtained at 2 K for a polycrystalline sample of $SmNiAl_4Ge_2$.

important tests. First, the hysteresis loop does not shift in position as a function of applied field during cooling of the sample, and the AC measurements show absence of frequency dependence of the susceptibility peak. From the saturation value a magnetic moment of 0.28 μ_B per formula unit can be calculated which is much lower than what would be expected from Sm^{3+} ions (0.80 μ_B) and is even lower than the expected value for Sm^{2+} ions (1.65 μ_B). Although the magnetic moment more suggests the presence of Sm^{3+} than Sm^{2+} ions, the reason for the low μ_{eff} value is probably due to the fact that the magnetization at 10 000 Gauss is not fully saturated. In this context, we point out that Sm magnetism, in general, is complicated and not well understood, and often the experimental values of magnetic moments in its corresponding compounds deviate substantially from the calculated values.[19] The contribution of Ni to the magnetic moment is thought to be negligible as has been determined in other rare earth/Ni compounds as well. This is the case, for example, in many $LnNiT_2$ compounds (Ln = rare earth metal, T = Si, Ge) which were studied by neutron diffraction.[20]

Experimental Section

The following reagents were used as obtained: Sm, 99.9%, metal chips, Research Chemicals, Phoenix, AZ; Y, 99.9%, −40 mesh, Cerac, Milwaukee, WI; Ni powder, 99%, Sargent; Ge, 99.999%, 3−6 mm pieces, Cerac.

Synthesis. $SmNiAl_4Ge_2$ was prepared by the reaction of 0.0150 g (1×10^{-4} mole) of Sm metal, 0.059 g (1×10^{-4} mole) of Ni metal, 0.0270 g (15×10^{-4} mole) of Al metal, and 0.0363 g (5×10^{-4} mole) of Ge mixed in an alumina tube. This tube was then sealed in an evacuated (1.0×10^{-4} Torr) 13 mm o.d. × 11 mm i.d. quartz tube and heated at 800° for 4 days, and then cooled at a rate of −6.25 °C/h to 500 °C and then −50 °C/h to 50 °C. The product was isolated in ~5 M NaOH and washed and dried with excess acetone and ether. This reaction

Table 1. Atomic Coordinates and Equivalent Isotropic Displacement Parameters ($A^2 \times 10^3$) for $MNiAl_4Ge_2$ (M = Sm, Y)[a]

	position	*x*	*y*	*z*	*U*(eq)[b]
Sm(1)	3a	0	0	0	6(1)
Y(1)		0	0	0	3(1)
Ge(1)	6c	−0.3333	0.3333	0.575(1)	6(1)
		−0.3333	0.3333	0.567(1)	9(1)
Ni(1)	6c	−0.3333	0.3333	−0.1667	4(1)
		−0.3333	0.3333	−0.1667	7(1)
Al(1)	6c	−0.3333	0.3333	0.1444(1)	9(1)
		−0.3333	0.3333	0.1441(2)	9(1)
Al(2)	6c	0.3333	−0.3333	0.889(1)	9(1)
		0.3333	−0.3333	0.886(2)	10(1)

[a] Each first line is for M = Sm; each second line is for M = Y. [b] *U*(eq) is defined as one-third of the trace of the orthogonalized *Uij* tensor.

Table 2. Bond Lengths [Å] and Bond Angles [deg] for $MNiAl_4Ge_2$ (M = Sm, Y)

	M = Sm	M = Y	
bond distances (Å)			
M(1)−M(1)	4.112	4.096	6×
M(1)−Ge(1)	2.9733(5)	2.9445(12)	6×
Ge(1)−Al(2)	2.5664(8)	2.563(2)	3×
Ge(1)−Al(1)	2.702(2)	2.707(5)	
Ni(1)−Al(2)	2.420(2)	2.418(5)	2×
Ni(1)−Al(1)	2.4731(6)	2.466(2)	6×
Al(1)−Al(1)	2.749(2)	2.746(5)	3×
Al(1)−Al(2)	2.9362(13)	2.924(4)	3×
bond Angles (deg)			
Ge(1)−M(1)−Ge(1)	180.0	180.0	3×
Ge(1)−M(1)−Ge(1)	87.50(2)	88.14(4)	6×
Ge(1)−M(1)−Ge(1)	92.50(2)	91.86(4)	6×
Al(2)−Ni(1)−Al(2)	180.0	180.0	
Al(2)−Ni(1)−Al(1)	73.74(4)	73.55(11)	6×
Al(2)−Ni(1)−Al(1)	106.26(4)	106.45(11)	6×
Al(1)−Ni(1)−Al(1)	112.48(3)	112.32(10)	6×
Al(1)−Ni(1)−Al(1)	67.52(3)	67.68(10)	6×
Al(1)−Ni(1)−Al(1)	180.0	180.0	3×
Al(2)−Ge(1)−Al(2)	106.48(4)	106.09(12)	3×
Al(2)−Ge(1)−Al(1)	67.68(4)	67.33(11)	3×
Al(2)−Ge(1)−M(1)	81.91(3)	81.90(8)	6×
Al(2)−Ge(1)−M(1)	165.30(5)	166.10(12)	3×
Al(1)−Ge(1)−M(1)	127.014(11)	126.57(3)	3×
M(1)−Ge(1)−M(1)	87.50(2)	88.14(4)	3×
Ni(1)−Al(1)−Ni(1)	112.48(3)	112.32(10)	3×
Ni(1)−Al(1)−Ge(1)	106.26(4)	106.45(11)	3×
Ni(1)−Al(1)−Al(1)	56.24(2)	56.16(5)	6×
Ni(1)−Al(1)−Al(1)	133.47(9)	133.0(3)	3×
Ge(1)−Al(1)−Al(1)	120.26(6)	120.6(2)	3×
Al(1)−Al(1)−Al(1)	96.84(7)	96.4(2)	3×
Ni(1)−Al(1)−Al(2)	123.57(2)	123.67(7)	6×
Ge(1)−Al(1)−Al(2)	53.96(4)	53.98(11)	3×
Al(1)−Al(1)−Al(2)	86.98(3)	87.18(10)	6×
Al(1)−Al(1)−Al(2)	174.22(8)	174.5(3)	3×
Ni(1)−Al(1)−Al(2)	52.31(3)	52.47(9)	3×
Al(2)−Al(1)−Al(2)	88.89(5)	88.9(2)	3×
Ni(1)−Al(2)−Ge(1)	112.32(4)	112.67(11)	3×
Ge(1)−Al(2)−Ge(1)	106.48(4)	106.10(12)	3×
Ni(1)−Al(2)−Al(1)	53.96(4)	53.98(11)	3×
Ge(1)−Al(2)−Al(1)	126.69(2)	126.86(5)	6×
Ge(1)−Al(2)−Al(1)	58.36(3)	58.69(9)	3×
Al(1)−Al(2)−Al(1)	88.89(5)	88.9(2)	3×

(19) (a) Carlin, R. L. In *Magnetochemistry*; Springer-Verlag: Berlin, 1986. (b) *Theory Appl. Mol. Paramagn.*; Boudreaux, E., Ed.; Wiley: New York, 1976; pp 257−270.

(20) Gil, A.; Szytula, A.; Tomkowicz, Z.; Wojciechowski, K. *J. Magn. Magn. Mater.* **1994**, *129*, 271−278 and refs 7 and 8 therein.

gave black powder and small silver-colored plates in 26% yield, based on Sm. Purity was measured by comparison of experimental powder patterns, both powder and plates, to theoretical calculated patterns. Purity was shown to be ~95% with the impurity peaks being due to residual elemental Ge.

$YNiAl_4Ge_2$ was prepared in a similar manner as the Sm compound.

Crystallography. $SmNiAl_4Ge_2$ crystallizes in the rhombohedral space group $R3m$ (no. 166) with cell dimensions: a = 4.1121(6) Å, c = 31.109(6) Å, V = 455.55(13) Å^3, Z = 3, and d_{calc} = 5.054 g/cm^3. A Rigaku AFC6S four-circle diffractometer was used to collect data from a crystal of 0.12 × 0.08 × 0.16 mm dimensions with Mo Kα (λ = 0.71069 Å^3) radiation. An empirical absorption correction based on ψ scans was applied to the data. Crystal data at 25 °C: μ(Mo Kα) = 22.816 mm^{-1}, 2θ range 5−59.92°, index ranges $-5 \le h \le 5$, $-5 \le k \le 5$, $-42 \le l \le 42$, total data 1744, unique data 207 (R_{int} = 0.0262), 205 reflections with $I > 2\sigma(I)$, no. of variables 15. Complete anisotropic refinement resulted in $R1/wR2$ = 1.21%/3.78% for reflections greater than $2\sigma I$, and $R/wR2$ = 1.83%/12.60% for all data, max peak in electron density map = 1.01 e$^-$ Å^{-3}, yielding a GOF = 0.888. The structure was solved with direct methods using SHELXS 86[21] and refined with SHELXS 5.03.

$YNiAl_4Ge_2$ crystallizes in the rhombohedral space group $R3m$ (no. 166) with cell dimensions: a = 4.0959(11) Å, c = 30.958(11) Å, V = 449.18(2) Å^3, Z = 3, and d_{calc} = 5.054 g/cm^3. A Siemens Platform CCD Diffractometer was used to collect data from a crystal of 0.2 × 0.2 × 0.16 mm dimensions with Mo Kα (λ = 0.71069) radiation. The SMART software was used for the data acquisition and SAINT for the data extraction and reduction. Crystal data at 25 °C: μ(Mo Kα) = 7.681 mm^{-1}, 2θ range 1.97−28.15°, index ranges $-5 \le h \le 5$, $-5 \le k \le 5$, $-40 \le l \le 38$, total data = 1456, unique data = 117 (R_{int} = 0.1110), 176 reflections with $I > 2\sigma(I)$, no. of variables = 15. Complete anisotropic refinement resulted in $R1/wR2$ = 4.64%/12.85% for reflections greater than $2\sigma(I)$, and $R/wR2$ = 4.70%/12.89% for all data, max peak in electron density map = 2.576 e$^-$ Å^{-3}, yielding a GOF = 1.270. The structure solution and refinements were preformed using the $SmNiAl_4Ge_2$ solution as a guide within the SHELXTL package of crystallographic programs. The coordinates of all atoms, isotropic temperature factors, and their estimated standard deviations for both compounds are given in Table 1. The selected bond distances and angles are given in Table 2.

Magnetic Susceptibility. The magnetic susceptibilities for $SmNiAl_4Ge_2$ and $YNiAl_4Ge_2$ were measured over the range 2−300 K using an MPMS Quantum Design SQUID magnetometer. Sample was ground to a fine powder to minimize possible anisotropic effects and loaded into poly(vinyl chloride) (PVC) containers. The temperature-dependent susceptibility studies were performed at 200 G. Corrections for the diamagnetism of the sample containers were made by measuring the magnetic response of the empty container under the same conditions of temperature and field which were measured for the filled container. Diamagnetic contribution of every ion to χ_M was corrected according to Selwood.[22]

Acknowledgment. This work made use of the W. M. Keck Microfabrication facility at MSU, an NSF MRSEC facility. The Siemens SMART platform CCD diffractometer was purchased with funds from the National Science Foundation (CHE-9634638). This work made use of the SEM facilities of the Center for Electron Optics at Michigan State University.

Supporting Information Available: Crystallographic refinement information for $SmNiAl_4Ge_2$ and $YNiAl_4Ge_2$. This material is available free of charge via the Internet at http://pubs.acx.org.

CM990155+

(21) (a) Sheldrick, G. M. In *Crystallographic Computing 3*; Sheldrick, G. M., Kruger, C., Doddard, R., Eds.; Oxford University Press: Oxford, England, 1985; pp 175−189.(b) SHELXTL: Version 5, 1994, Sheldrick, G. M.; Siemens Analytical X-ray Systems, Inc., Madison, WI.

(22) Selwood, P. W. *Magnetochemistry*, 2nd ed.; Interscience Publishers: New York, 1956.